**THE EUROPEAN
PHYSICAL JOURNAL C**

CrossMark

Regular Article - Theoretical Physics

Upgrading sterile neutrino dark matter to FImP using scale invariance

Zhaofeng Kang[a]

School of Physics, Korea Institute for Advanced Study, Seoul 130-722, Korea

Abstract In this article we propose a class of extremely light feebly interacting massive particle, FImPs. They are combination of feebly interacting massive particle with scale invariance, by which DM stability, mass origin and relic density are inherently related. In the scale invariant version of the Standard Model (SM) with three right-handed neutrinos (νSISM), the lightest N_1 realizes the FImP scenario. In this example scalar singlets, which are intrinsic to the νSISM, generate mass and relic density for this FImP simultaneously. Moreover, they are badly needed for electroweak symmetry spontaneously breaking. Interestingly, a 7.1 keV N_1 with correct relic density, which can explain the recent 3.55 keV X-ray line, lies in the bulk parameter space of our model.

1 Introduction and motivation

The existence of dark matter (DM) is commonly believed in; nevertheless, its particle properties are still in the dark. The hypothesis that DM is a weakly interacting massive particle (WIMP) prevails, mainly due to the so-called WIMP miracle, which says that if DM annihilates involving weak scale mass and strength, it will obtain the correct order of magnitude for relic density $\Omega_{\rm DM} h^2 \sim 0.1$. Despite a lot of experimental efforts made (including (in)direct DM detections and also collider searches), one still has not detected any trace of DM with confirmation. These null results [1] begin to challenge the WIMP paradigm.

Now it is the right time to reexamine the theoretical basis of WIMP DM and explore other DM frameworks, or more concretely, models. We would like to follow the ensuing basic questions about DM.

- First, why is it there? A DM candidate that is predicted rather than introduced would be more attractive. A good case in point is the lightest sparticle in SUSY and the axion from the Peccei–Quinn models aiming at solving the strong CP problem. Another example is the core of this paper, the lightest right-handed neutrino (RHN) N_1, or sterile neutrino [2]. Originally RHNs are introduced to explain the nonzero neutrino masses, but they are neutral and thus have potential to provide a DM candidate.

- Second, why is it stable (or at least sufficiently long-lived on a cosmic time scale)? Again, we advocate a mechanism that naturally guarantees DM stability rather than imposing a protective symmetry like Z_2 by hand. For instance, such a Z_2 may be an accidental symmetry due to the field content along with the space-time and gauge symmetries of the model, see an example based on scale invariance (SI) [3,4],[1] a symmetry which may address the hierarchy problem [5–31]. Sterile neutrino DM offers another line for stability: lightness along with feebly interactions. No exact symmetry, by hand or accidental, is invoked here, and thus DM is expected to decay, say, into the very light SM species like neutrino and photons. But the decay rate is greatly suppressed by powers of DM mass and couplings, so DM can be sufficiently long-lived.

- Last but not the least, why is the DM relic density $\Omega_{\rm DM} h^2$ around 0.1? The WIMP scenario presents the WIMP miracle.[2] We find that a similar numerical coincidence may also arise in the framework of feebly interacting massive particle (FIMP) [32,33]. Moreover, it is tied to the mass origin and stability of DM.

Let us neglect the first question for the time being. The answer to the second and third questions may point to a

---

[1] Under some reasonable assumptions one concludes that the only viable accidental DM (aDM) must be a singlet scalar. But this paper is restricted to WIMP. Beyond it, a singlet fermion N is also viable provided that its coupling to the visible sector is sufficiently weak, namely $y_N \bar{\ell} \Phi N$ with $y_N \ll 1$. For N introduced in this way is naturally identified with the lightest RHN.

[2] In practice, a lot of WIMP dark matters studied recently are far away from this miracle.

[a] e-mail: zhaofengkang@gmail.com

Springer

framework which combines FIMP with SI. The FIMP DM X (e.g., a Majorana fermion like N_1) feebly interacts with other fields, including the Higgs-like field $\mathcal{S}$, which generates its mass via the term $\mathcal{S}X^2$, so it will be very light as long as the vacuum expectation value (VEV) of $\mathcal{S}$ is not hierarchically above TeV. Lightness plus feeble interactions are appropriate to give accidentally long-lived DM. Additionally, that mass source term can simultaneously freeze-in FIMP with correct relic density. Hereafter that kind of FIMP is dubbed FImP with "m" indicating its lightness due to SI. Needless to say, FImP cannot be seen by the current DM detectors, except for these sensitive to X-ray. We mention that, with regard to experimental tests, FImP, which tends to produce X-ray, is more interesting than FIMP, which usually stays in the dark.

The FImP example N_1 from the νSISM is of special interest, because it gives answers to all those three questions. Interestingly, there are some suggestive hints which favor such DM in the X-ray line at energy 3.55 keV, which was reported recently and can be explained by the 7.1 keV N_1 with active–sterile neutrino mixing angle $\simeq 0.8 \times 10^{-5}$ [34,35]. Despite the difficulty existing in the conventional ways, such a N_1 can easily get a correct relic density via freeze-in [36–38]. In this paper we will concentrate on the N_1 example, and another interesting example based on scalar FImP is considered in Appendix C.

In a later stage of this paper, we found that the idea of introducing a scalar singlet to freeze-in N_1 has already been explored by several groups [39–42]. Even then, there are several obvious differences between our paper and theirs. First of all, only in this paper the singlet is a built-in rather than artificial ingredient. Second, only here the singlet plays a crucial role in EWSB, while in others it is just a spectator. EWSB will be one of the centers of our article. Third, only here N_1 could enjoy the merits of FImP. Last but not least, we actually will need two scalar singlets for the sake of successful EWSB with acceptable Higgs phenomenologies, and this will make a difference in freeze-in.

The paper is organized as follows. In Sect. 2 we introduce the νSISM, studying EWSB, the mass spectrum, and freeze-in dynamics. We present the numerical results in Sect. 3, and the next section includes a conclusion and a discussion. Finally, some supplementary materials are in the appendix.

2 The scale invariant version of νSM (νSISM)

As stated in the Introduction, the νSISM predicts the FImP DM N_1, which takes advantage in addressing the basic properties of DM such as mass and relic density origins and stability. In this section we will first introduce the model and then study its two main phenomenologies, SI spontaneously breaking and the N_1 freeze-in production. The scalar singlets will play crucial roles in both aspects.

We begin with the model setup. Asides from the SM field content, the νSISM introduces three RHNs, N_i, to produce realistic neutrino masses and mixings. However, in order to generate Majorana masses for N_i, scalar singlets, $S_a (a = 1, 2 \ldots n)$, with non-vanishing VEVs are indispensable. Interestingly, they are also badly needed to implement radiative SI spontaneously breaking. It is found that the minimal case with $n = 1$ fails to accommodate the current Higgs data [43,44], so we consider $n = 2$ real scalars or a complex singlet $S = (J + i\sigma)/\sqrt{2}$. These minimal degrees of freedom are subject to the $SU(3)_C \times SU(2)_L \times U(1)_Y$ gauge symmetries and the Poincaré and classical scale invariance space-time symmetries. Then the most general interacting Lagrangian reads

$$-\mathcal{L} = \frac{\lambda_1}{2}|H|^4 + \frac{\lambda_2}{2}|S|^4 + \lambda_3 |H|^2 |S|^2 \\ + \left(\lambda_4 |H|^2 S^2 + \lambda_5 S^3 S^* + \frac{\lambda_6}{2} S^4 + c.c. \right) \\ + \left(\frac{\lambda_{sn}}{2} SN^2 + y_N \bar{\ell} H N + c.c. \right). \tag{1}$$

To reduce parameters, we also impose CP-invariance on the scalar potential, which forces $\lambda_{4,5,6}$ to be real. But this symmetry is not physically necessary (we allow a complex Yukawa coupling to break it explicitly). For later use the expansion of Eq. (1) in real degrees of freedom is given in Appendix A.

A comment about the novelty of the νSISM is in order. As a matter of fact, it is not entirely new and similar versions have been investigated in Refs. [43–45]. However, our physical motivations and the arguments of the model presented here are quite different from theirs. In addition to that, our focused parameter space will be totally different.

2.1 Scale invariance spontaneously breaking

2.1.1 Flat direction and tree level spectrum

We proceed to investigate the vacuum of the scalar potential given in Eq. (1). In the absence of a symmetry, it is supposed that both components of S develop VEVs. So, along with the Higgs doublet VEV, we should work in the three-dimensional field space. The treatment of such a situation becomes more complicated than the single field case, and the Gildener–Weinberg [46] instead of the Coleman–Weinberg (CW) [47] approach is appropriate. Following this approach, we should work out the flat directions of the scalar potential, namely $\vec{\Phi}_{\text{flat}} = \varphi \vec{n}$ with φ and $\vec{n}$, respectively, the modular and directional vector of $\vec{\Phi}_{\text{flat}}$ in the multi-dimensional field space. The existence of such a kind of directions is a consequence of SI at tree level, which leads to the modular-independent minimum lines of the potential, i.e., the lines

satisfying the equation $dV_{\text{tree}}/d\varphi = 0$. The flat directions will be lifted by radiative corrections that introduce sources of SI violation and then fix the value of φ. We recall that these operations are employed at the renormalization scale Q, at which all couplings are inputted. Later, it will be chosen at the SI spontaneously breaking scale.

We have simplified the potential by imposing CP-invariance, and this simplification allows us to obtain analytical expressions of the flat direction (and mass spectrum as well). Such a strategy is also adopted in Ref. [45], but it further imposes a Z_4 discrete symmetry to eliminate the λ_4- and λ_5-terms. The flat direction is the solution of the following three tadpole equations:

$$\frac{J^2}{h^2} = y^2, \tag{2}$$

$$\lambda_J + 3\frac{\lambda_{hJ}}{y^2} + 3x^2\lambda_{J\sigma} = 0, \tag{3}$$

$$x^3\lambda_\sigma + 3x\frac{\lambda_{h\sigma}}{y^2} + 3x\,\lambda_{J\sigma} = 0, \tag{4}$$

where we have introduced two VEV ratios $x \equiv \sigma/J$ and $y \equiv J/h$. As a convention, we always choose J as the largest scale and thus $y > 1$ (we will turn back to it later). The above equations are derived from the potential expressed in terms of real components; see Eq. (A2) and the definitions of coupling constants Eq. (A3). Immediately, from these equations one can see that in the Z_4-symmetric case, where $\lambda_4 = \lambda_5 = 0$ and thus $\lambda_J = \lambda_\sigma$, $\lambda_{hJ} = \lambda_{h\sigma}$, only solutions $x = \pm 1$ are possible. In other words, Z_4 forces the flat direction to lie along the special direction $\sigma = J$. But more generic flat directions can be admitted in the absence of such a symmetry. The resulting Higgs physics is different.

In our later numerical demonstration, the VEV ratios x and y will be taken as fixed inputs, since they have direct physical meaning. Note that y can be expressed in terms of x and other quartic coupling constants,

$$y^{-2} = -3\frac{\lambda_{hJ} + x^2\lambda_{h\sigma}}{\lambda_h}. \tag{5}$$

In all cases of interest we shall find that y is at least moderately larger than 1, and thus there should be a mild hierarchy, i.e., $\lambda_{hJ}, \lambda_{h\sigma} \ll \lambda_h$. Otherwise we have to arrange a cancellation between the two terms in the numerator. It is convenient to express the flat direction in terms of x, y, and h as follows:

$$\varphi = R(x, y)h \quad \text{with} \quad R^2(x, y) = 1 + y^2 + x^2y^2, \tag{6}$$

$$n_h = \frac{1}{R(x, y)}, \quad n_J = \frac{y}{R(x, y)}, \quad n_\sigma = \frac{xy}{R(x, y)}. \tag{7}$$

By definition, we have the relations $v_{h,J,\sigma} = n_{h,J,\sigma}\varphi$. Later we will find that $R(x, y)$ (or n_h) has a clear interpretation.

The tree level spectrum along the above flat direction consists of three Higgs states, the Goldstone boson (GSB) of SI spontaneously breaking $\mathcal{P}$ and two massive states $H_{1,2}$. We should calculate radiative corrections of the tree level potential due to these states. The mixings between these scalars are largely determined at tree level. Concretely, the three states are obtained from the mass squared matrix M^2, which in the basis (h, J, σ) takes the form of

$$M^2 = \frac{J^2}{y^2} \times \begin{pmatrix} \frac{\lambda_h}{3} & \frac{\lambda_h}{3y} + x^2y\,\lambda_{h\sigma} & -x\,y\,\lambda_{h\sigma} \\ \frac{\lambda_h}{3y^2} + x^2\lambda_{h\sigma} - x^2y^2\lambda_{J\sigma} & x\,y^2\,\lambda_{J\sigma} \\ & -\lambda_{h\sigma} - y^2\lambda_{J\sigma} \end{pmatrix}. \tag{8}$$

We have expressed λ_J and λ_σ in favor of others via the tadpole conditions Eqs. (3) and (4), respectively. One can explicitly check that $\text{Det}M^2 = 0$, hence implying a GSB.

The two massive Higgs bosons can be analyzed in a simple way. The Higgs sector must present a quite SM-like Higgs boson h_{SM}, which must be dominated by the Higgs doublet, merely containing small fractions of singlets. It means that the Higgs sector can be split into a doublet sector and a singlet sector. In this simplified case, the singlet sector breaks SI through large singlet VEVs, which are then directly mediated to the doublet sector through the mixing term $S^2|H|^2$, generating the negative Higgs mass term for EWSB.[3] Now, the mass squared of h_{SM} can be approximated by

$$m_{h_{\text{SM}}}^2 = m_{H_1}^2 \approx M_{11}^2 = \frac{\lambda_h}{3}v^2. \tag{9}$$

So as usual $\lambda_h \approx 0.75$ is almost fixed by the 125 GeV Higgs boson, up to a small correction from the mixing effect. With this result and taking into account the presence of a GSB, which is dominated by singlets, it is not difficult to deduce the mass squared of the heavier Higgs boson H_2:

$$m_{H_2}^2 \approx M_{22}^2 + M_{33}^2$$
$$= -[(1 + x^2)\lambda_{J\sigma} + (1 - x^2)\lambda_{h\sigma}/y^2]v_J^2. \tag{10}$$

In the ensuing discussion we will see that, to guarantee the presence of h_{SM}, at least one singlet should develop a larger VEV than that of the doublet, v. As mentioned before in our notation we take $v_J = \langle J \rangle \gg v$ or $y = v_J/v \gg 1$. Then the mass of H_2 is well approximated by

$$m_{H_2} \approx \sqrt{-(1 + x^2)\lambda_{J\sigma}}v_J. \tag{11}$$

---

[3] In this sense, it actually reduces to the Higgs portal-like models with hidden CW mechanism [11–17].

Or one can express it in terms of v_φ, $m_{H_2} = x\sqrt{\frac{\lambda_\sigma}{3} + \frac{\lambda_{h\sigma}}{x^2 y^2}}$ v_φ, by solving $\lambda_{J\sigma}$ from Eq. (4). In most cases it can be further approximated to be of the very simple form $x\sqrt{\lambda_\sigma/3}v_\varphi$.

2.1.2 CW potential and pseudo-GSB mass

With the massive spectrum at hand, we now discuss SI spontaneous breaking in the one loop CW effective potential V_{CW}. In general, it can be written as [45]

$$V_{CW} = A(\vec{n})\varphi^4 + B(\vec{n})\varphi^4 \ln \frac{\varphi^2}{Q^2}. \tag{12}$$

The numerical factors A and B are functions of the dimensionless couplings only. In the MS scheme, they are explicitly given by

$$A = \frac{1}{64\pi^2}\left[\sum_s g_s^4(-3/2 + \ln g_s^2) + 3\sum_V g_V^4(-5/6 + \ln g_V^2)\right.$$
$$\left. -4\sum_f g_f^4(-1 + \ln g_f^2)\right],$$
$$B = \frac{1}{64\pi^2}\left(\sum_s g_s^4 + 3\sum_V g_V^4 - 4\sum_f g_f^4\right), \tag{13}$$

with $s/V/f$ denoting real scalar/vector boson/Dirac fermion, respectively. In writing these expressions, we have collectively assumed the relation $m = gv_\varphi$, which is true in the models with SI. It is worthy of note that in the multidimensional field space, if the field that gains mass mainly via coupling to the scalar with a smaller VEV, e.g., h in this context, the resulting effective coupling g will be suppressed by the fraction $n_h \ll 1$. In this way, we can avoid the failure of the scale invariant SM, which is caused by the large negative contribution to B from the heavy top quark. We will come back to this point later.

Within the perturbative region, namely both A and B much smaller than 1, the VEV of φ is pinned down by solving the equation $dV_{CW}/d\varphi = 0$. From this we get the relation

$$v_\varphi = Q \exp(-A/2B - 1/4). \tag{14}$$

If we choose $Q = v_\varphi$, which eliminates the potential large logarithmic terms, we get a relation among the couplings at scale Q, i.e., $A + 2B = 0$. It is nothing but the phenomenon of dimensional transmutation [47]. Perturbativity of the effective potential is satisfied for $g_s \lesssim 1$. If both A and B receive contributions mainly from a single field dependent mass term, such as m_{H_2} in this paper, we can approximately determine the effective coupling constant to be

$$g_s \approx \sqrt{e}\, Q/v_\varphi, \tag{15}$$

or $m_s = \sqrt{e}\,Q$. Equation (15) tells that, if we choose $Q \gg v_\varphi$, then $g_s \gg 1$, and thus it violates perturbativity at Q. In the opposite case, one may want to choose $Q \ll v_\varphi$ to get a weak coupling $g_s \ll 1$. But it will result in an intolerably light PGSB with mass suppressed by Q/v_φ (or g_s). Therefore, $g_s \sim \mathcal{O}(1)$ is preferred. This fact is useful to find the favored region of x. Recall that $m_{H_2} = x\sqrt{\lambda_\sigma/3}v_\varphi$ (see remarks below Eq. (11)); thus we have $g_{H_2} \approx x(\lambda_\sigma/3)^{1/2}$. Then to make $g_s \equiv g_{H_2} \sim 1$ we need $\lambda_\sigma \sim 3/x^2$, but it blows up even for $x \lesssim 0.3$. So the vacuum figuration with $x \lesssim 1$ is favored, which means that H_2 tends to a strong mixture of σ and J.

Now we turn our attention to the pseudo GSB (PGSB), $\mathcal{P}$, which is massless at tree level but gets a mass from the effective potential. Before heading toward its mass, we would like to first figure out its doublet fraction $F_{\mathcal{P}h}$, which is useful in constraining/discovering this PGSB at colliders. After an explicit calculation, one finds that this fraction is nothing but just the doublet projection in the tree level flat direction, see Eq. (6),

$$F_{\mathcal{P}h} = n_h = 1/R(x, y) \ll 1, \tag{16}$$

up to an overall sign. $F_{\mathcal{P}h}$ is determined solely by the VEV ratios x and y. A small $F_{\mathcal{P}h}$ is necessary not only to hide a fairly light PGSB at LEP but also to keep h_{SM} overwhelmingly dominated by the doublet. To sufficiently suppress it, at least one of the singlet VEVs should be significantly larger than v, i.e., $y \gg 1$ and/or $xy \gg 1$. Following the previous convention, we take $y \gg 1$ and then we have $F_{\mathcal{P}h} \approx 1/y\sqrt{1 + x^2}$. Note that in this convention $x \leq 1$, thus $xy \gg 1$ also means $y \gg 1$.

The classical SI is violated by quantum effect which thus generates a mass for the tree level massless GSB. In general, it is given by

$$m_{\mathcal{P}}^2 = 8Bv_\varphi^2$$
$$= \frac{1}{8\pi^2}\left(\sum_s g_s^2 m_s^2 + 3\sum_V g_V^2 m_V^2 - 4\sum_f g_f^2 m_f^2\right). \tag{17}$$

To ensure that the extremum from $dV_{CW}/d\varphi = 0$ is indeed a minimum, $m_{\mathcal{P}}^2$ or B must be positive. In the above expression, top quarks have the potential to drive $B < 0$ but it is stopped by H_2. The stability condition is

$$g_{H_2}^4 > 12g_t^4 \Rightarrow x^2\left(\frac{\lambda_\sigma}{3} + \frac{\lambda_{h\sigma}}{x^2 y^2}\right) > \frac{2\sqrt{3}(m_t/v)^2}{y^2(1 + x^2)}. \tag{18}$$

It is actually required that $\lambda_\sigma > 6.3/y^2 x^2 (1 + x^2)$. No surprise, when $x < 1/y \ll 1$ (or $x^2 y^2 \lesssim 1$), namely one of the singlet having VEV below the weak scale, that one needs a large $\lambda_\sigma \sim \mathcal{O}(10)$ to compensate for the relatively larger suppression by n_σ in g_{H_2} (compared to that by n_h in g_t). This is not an appealing situation if we want to keep the model perturbative up to a very high scale. Moreover, the resulting spectrum, in particular $\mathcal{P}$, is fairly light and thus may have already been excluded by the present experiments like LEP and LHC.[4] Therefore, we will focus only on the case $x^2 y^2 \gg 1$, consistent with the analysis below Eq. (15), which concludes that x should be near 1. In the H_2-dominance limit, after using Eq. (15), the PGSB mass is expressed in the following form:

$$
\begin{aligned}
m_\mathcal{P} &= \frac{g_s^2}{2\sqrt{2}\pi} v_\varphi = \frac{\lambda_\sigma/3 + \lambda_{h\sigma}/x^2 y^2}{2\sqrt{2}\pi} x^2 \sqrt{1 + x^2}\, yv \\
&\approx 0.038\, \lambda_\sigma\, x^2 \sqrt{1 + x^2}\, yv.
\end{aligned}
\tag{19}
$$

As an estimation, we write $m_\mathcal{P} = 75.7 \times (y/5.0)(\lambda_\sigma/2.0)$ GeV with $x = 0.8$ fixed. Increasing y helps to not only suppress the doublet fraction of $\mathcal{P}$ but also enhance the mass of $\mathcal{P}$, thus making it safe under the LEP exclusion. The price is pushing H_2 into the TeV region, thus making it hard to detect at near future colliders. But $\mathcal{P}$ is still promising. We leave more quantitative analysis in the coming section and in the ensuing subsection we enter into a discussion of dark matter, the FImP N_1.

2.2 Freeze-in sterile neutrino

Before heading toward the freeze-in production of sterile neutrino dark matter N_1, we briefly discuss its conventional production mechanisms. The tiny active neutrino mass leads to a naive upper bound on the Yukawa coupling constant given in Eq. (1) (the bound may be spoiled somehow in the presence of flavor structure),

$$
y_N \lesssim 10^{-10} \left(\frac{m_\nu}{0.1\,\mathrm{eV}}\right)^{1/2} \left(\frac{M_{N_1}}{10\,\mathrm{keV}}\right)^{1/2}.
\tag{20}
$$

That feeble coupling means that N_1 never enters the thermal plasma, given no other interactions. It can be nonthermally produced via non-resonant sterile-active neutrino oscillation, known as the Dodelson–Widrow (DW) mechanism [48]. But it has been ruled out (we will give reasons later). The resonant production [49] and thermal production mechanisms [50] are still allowed. However, both suffer some

theoretical defects since they require big modifications. The former requires an anomalously large lepton asymmetry, and the latter requires a large entropy release. Model extensions are then unavoidable.[5]

In the νSISM, new interactions of N_1 with the singlets appear naturally. These new interactions originally are supposed to generate very light mass for N_1 (lightness is necessary for stability), but at the same time they surprisingly can account for the correct relic density of N_1 via the freeze-in mechanism.

2.2.1 A toy analysis

As a toy analysis, only one singlet is considered for the time being. For the keV scale N_1, again for stability (and for cosmological considerations [51]), the strength of the coupling is extremely small $\lambda_n \sim 10^{-8}$. Hence this new vertex cannot thermalize N_1 either. But the magnitude of λ_n is just at the correct order to admit freeze-in production of N_1. In this scenario, N_1 is produced via the slow decay process $S \to N_1 N_1$, which has a negligible inverse decay rate. Note that generically the annihilation processes like $f\bar{f} \to \bar{N}_1 N_1$ contribute to the freeze-in process sub-dominantly [52,53], due to the reason, among others, that they are suppressed by extra small couplings. The freeze-in process lasts until the mother particle decouples from the plasma and quickly decays away. The peak of production is around the mass scale of the mother particle S. In other words, it is UV-insensitive (for UV-sensitive freeze-in, please see Ref. [54]). For freeze-in proceeding via two-body decay $P \to \bar{X}X$, the final yield of X is formulated to be [32,33,52,53,55,56]

$$
Y_X(\infty) \approx \frac{45\, g_P}{1.66\pi^4 g_*^S \sqrt{g_*^\rho}} \frac{\Gamma(7/2)\Gamma(5/2)}{16} \frac{M_\mathrm{Pl}}{m_P^2} \Gamma(P \to \bar{X}X),
\tag{21}
$$

with $g_*^{S,\rho}$, respectively, the effective numbers of degrees of freedom for the entropy and energy densities at $T \simeq m_P$, the mass of the mother particle. g_P is the number of internal degrees of freedom of P. For multiple mother particles contributing to freeze-in X, there is a summation over P. Specified to this schematic example for freeze-in N_1, the relic density depends on the unknown parameters as proportional to $\lambda_n^3 \langle S \rangle$. Then, for a TeV scale $\langle S \rangle$, it is found that a keV scale FImP allows for correct relic density. This kind of feeble interaction admitting a correct relic density of extremely light DM is somewhat reminiscent of a weak interaction admitting the correct relic density of the weak

---

[4] Practically such a VEV pattern will make for freeze-in RHN in the single RHN limit, and at some corner of the parameter space the light Higgs bosons are also allowed. But we only consider the bulk space, with clear and safe Higgs phenomenologies.

[5] If the two heavier RHNs have quasi-degenerate masses, typically with degeneracy $\lesssim 10^{-4}$, they are even capable of generating the observed baryon asymmetry of the Universe [66]. But generically it implies a large fine-tuning.

scale DM. Here the TeV scale, a sign of new physics, is also involved, but it is in the form of a VEV rather than the DM mass scale itself.

The analysis in the realistic model becomes more complicated in two respects. First, there are two singlets J and σ coupling to N_1, both having VEVs. Moreover, two physical Higgs bosons $\mathcal{P}$ and H_2 (actually three but the contribution from the SM-like Higgs boson is suppressed by small mixing) contribute to the freeze-in process. Second, it is well known that a single family of RHN fails to accommodate neutrino phenomenologies, and thus a nontrivial flavor structure should be taken into account. This, along with the multi singlets, is going to make a big difference. We find that there are two distinguishable scenarios that can successfully freeze-in N_1, and one of them is just reduced to the single RHN case.

2.2.2 Consider multi-singlets and flavor structure

As a warm up, we consider the case with only one RHN N_1 but two singlets. The Lagrangian relevant to freeze-in is derived as follows:

$$\frac{\eta_{S_\alpha}}{2} S_\alpha N_1 N_1 \rightarrow \frac{M_{N_1}}{2} N_1^2 + \frac{\eta_{H_a}}{2} H_a N_1 N_1,$$
$$\eta_{H_a} \equiv \sum_\alpha \eta_{S_\alpha} F_{S_\alpha H_a}, \tag{22}$$

with $S_\alpha = (J, \sigma)$ and $M_{N_1} = \eta_{S_\alpha} v_{S_\alpha} = (x\,\eta_J + \eta_\sigma) v_\sigma$.[6] We have written $S_\alpha = F_{S_\alpha H_a} H_a$ with $H_a = (\mathcal{P}, H_1, H_2)$. In the region of interest with $x \lesssim 1$ and $y \gg 1$, the H_1 ($= h_{\mathrm{SM}}$) component can be neglected. Other fractions are approximately parameterized by one mixing angle θ between the singlets: $F_{J\mathcal{P}} = F_{\sigma H_2} = \cos\theta$ and $-F_{JH_2} = F_{\sigma\mathcal{P}} = \sin\theta$ with $\tan\theta = x$ and $\theta \in [0, \pi/4]$. It is illustrative to write $\eta_{H_a} = f_{H_a} M_{N_1}/v_J$ with

$$f_{\mathcal{P}} = \left[1 + \frac{v_J}{M_{N_1}}(1 - x^2)\eta_J\right]\cos\theta,$$
$$f_{H_2} = \frac{1}{x}\left(1 - 2x\frac{v_\sigma}{M_{N_1}}\eta_J\right)\cos\theta. \tag{23}$$

Barring cancellation between the two contributions to M_{N_1}, one gets the naive estimations $\eta_{\sigma,J} \sim M_{N_1}/v_{\sigma,J}$. In particular, if only one singlet couples to N_1, there will be no cancellation and then for $x \simeq 1$ it is expected that $f_{H_\alpha} \sim 1$, the reference value for f_{H_α} hence. Now substituting the decay

width of $H_a \rightarrow N_1 N_1$ into Eq. (21) one can estimate the DM relic density $\Omega_{\mathrm{DM}} h^2 = 2.82 \times 10^2 (\frac{m_{\mathrm{DM}}}{\mathrm{keV}}) Y_{\mathrm{DM}}(\infty)$ as

$$\Omega_{\mathrm{DM}} h^2 = 0.11 \times \sum_{H_a = \mathcal{P}, H_2} \left(\frac{f_{H_a}^2}{1.0}\right) \left(\frac{m_{\mathrm{DM}}}{10\,\mathrm{keV}}\right)^3 \left(\frac{\mathrm{TeV}}{v_J}\right)^2$$
$$\times \left(\frac{100\,\mathrm{GeV}}{m_{H_a}}\right) \left(\frac{10^3}{g_*^S \sqrt{g_*^\rho}}\right), \tag{24}$$

with $m_{\mathrm{DM}} = M_{N_1}$.

From the above equation we find that there is a mild tension between the Higgs sector and the dark sector. The tension gets more serious as N_1 becomes lighter, e.g., as light as the potential warm dark matter with mass around 1 keV. For that light DM, Eq. (24) shows that the dark sector wants the singlets' VEV to lie significantly below the TeV scale, which, however, is disfavored by the Higgs phenomenology in terms of the previous discussions. Therefore, we may have to endure a substantial cancellation between the two singlets coupling to N_1, so as to make at least one $f_{H_a} \sim 10$. Immediately, we know that the case with only one singlet coupling to RHN fails in freezing-in a quite light N_1, because it always gives $f_{H_a} \sim 1$.

Now let us detail how incorporating the flavor structure for RHNs makes a big difference. Actually, it opens up a novel scenario for freeze-in. To see it, we consider a simplified case, i.e., there is a large mass hierarchy between the DM candidate and the extra RHNs; for instance, the other two RHNs lying at the GeV scale inspired by baryogenesis [66]. The genetic Yukawa couplings are $\eta_{S_\alpha,ij} S_\alpha N_i N_j/2 + c.c.$ with $\eta_{S_\alpha,ij} = \eta_{S_\alpha,ji}$ and $i/j = 1, 2, 3$. After writing $S_\alpha \rightarrow v_{S_\alpha} + S_\alpha$, we as usual can work in the mass eigenstates of RHNs through an unitary rotation $N_i \rightarrow U_{ij} N_j$ and eventually arrive at the Lagrangian

$$-\mathcal{L}_N = \frac{M_i}{2} N_i^2 + \frac{\eta_{H_a,ij}}{2} H_a N_i N_j + c.c., \tag{25}$$

with $M_{N_1} \ll M_{N_2} \leq M_{N_3}$ and $\eta_{H_a,ij} = F_{S_\alpha H_a}(U^\dagger)_{ii'} \eta_{S_\alpha,i'j'} U_{j'j}$. Owing to multi singlets with VEVs, the mass matrix and the Yukawa coupling matrix of RHNs cannot be diagonalized simultaneously. Consequently the interaction of N_1 is more involved than that of the previous case, which is only the limit of a negligible mixing effect in the case considered here. To understand this limit better and for later convenience, we come back to the original mass matrix M_N (for illustration only two RHNs are considered):

$$M_N = \begin{pmatrix} \eta_{J,11} v_J + \eta_{\sigma,11} v_\sigma & \eta_{J,12} v_J + \eta_{\sigma,12} v_\sigma \\ \eta_{J,12} v_J + \eta_{\sigma,12} v_\sigma & \eta_{J,22} v_J + \eta_{\sigma,22} v_\sigma \end{pmatrix}$$
$$\sim \begin{pmatrix} \mathcal{O}(10^{-6}) & \mathcal{O}(10^b) \\ \mathcal{O}(10^b) & \mathcal{O}(10^{2a}) \end{pmatrix} \mathrm{GeV}, \tag{26}$$

---

[6] The SM Higgs doublet also contributes to the mass of N_1 via the dimension-five operator $|H|^2 N_1^2/\Lambda$, which is obtained after integrating out the singlet S with VEV v_s and mass m_S. Roughly, $\Lambda \sim \lambda_{sh}\lambda_{sn} v_s/m_S^2 \sim \frac{\lambda_{sn}}{v_s}(m_h/m_S)^2$, where we have used the induced weak sale from $\lambda_{sh}|H|^2 S^2$. Therefore, compared to the contribution from S to N_1, $M_{N_1} \sim \lambda_{sn} v_s$, this contribution is suppressed by $(\frac{v}{v_s}\frac{m_h}{m_S})^2 \ll 1$.

with $-3 \lesssim a \lesssim 0$. To make the lighter eigenvalue naturally $\sim \mathcal{O}(10^{-6})$ GeV, b should be smaller than $a - 3$. The single RHN case discussed before corresponds to $b \ll a - 3$, a condition to decouple the heavy from the light.

On the contrary, when $b \lesssim a - 3$ the light–heavy RHN mixing effect is not negligible and can play an important role. Still we consider the hierarchical scenario, where the mixing angle is estimated to be $\sin \theta_N \simeq (M_N)_{12}/(M_N)_{22} \sim 10^{b-2a} \ll 1$. Two off-diagonal Yukawa coupling constants $\eta_{H_a,12}$, by naive estimation, are approximated to be

$$
\begin{aligned}
\eta_{H_a,12} &\approx F_{S_\alpha H_a}(\eta_{S_\alpha,11} \sin \theta_N \\
&\quad + \eta_{S_\alpha,12} - \sin^2 \theta_N \eta_{S_\alpha,21} - \sin \theta_N \eta_{S_\alpha,22}) \\
&\simeq F_{S_\alpha H_a}(\eta_{S_\alpha,12} - \sin \theta_N \eta_{S_\alpha,22}).
\end{aligned} \tag{27}
$$

After some exercise, it is not difficult to find that at leading order $\eta_{\mathcal{P},12} = 0$. But the one involving H_2 is not zero, and explicitly it is given by

$$
\begin{aligned}
\eta_{H_2,12} &\approx \cos \theta (\eta_{\sigma,12} - x \eta_{J,12}) \\
&\quad - \cos \theta (\eta_{\sigma,22} - x \eta_{J,22}) \frac{x \eta_{\sigma,12} + \eta_{J,12}}{x \eta_{\sigma,22} + \eta_{J,22}}.
\end{aligned} \tag{28}
$$

As one can see, $\eta_{H_2,12} \sim \eta_{S_\alpha,12} \sim 10^b/v_{S_\alpha}$. It is $b - 6$ orders of magnitude larger than $\eta_{H_a,11}$, which is expected to be $\sim 10^{-9}$ for a keV RHN. Recall that $b < a - 3$, thus as long as a is not less than -2, $\eta_{H_2,12}$ can easily be around 10^{-8}. In the light of the estimation in Eq. (24), this light–heavy mixing effect is able to freeze-in a quite light ($\sim$keV) N_1 via decay $H_2 \to N_1 N_2$. We stress again that the presence of multi singlet scalars is key to preserving a significant mixing effect $\eta_{H_a,12} \neq 0$. In summary, in our paper the correct relic density of N_1, no matter light or heavy, can be readily achieved by means of freeze-in.

3 The numerical analysis of the νSISM

In this section we investigate the numerical results of the Higgs and dark sectors phenomenologies, respectively. For the former, we are not interested in making a parameter space scan. Instead, we try to make the features of the Higgs boson spectrum visual. For the latter, we even are not concerned with the original parameters, since from the previous analysis it is known that the correct relic density of N_1 can always be achieved over a fairly wide region of M_{N_1}. So the dark matter phenomenologies actually involve only two parameters, M_{N_1} and $\sin \theta_1$, the mixing angle between N_1 and active neutrinos. Noticeably, the recently reported X-ray line at 3.55 keV can be readily explained by the decaying N_1 (7.1 keV DM with freeze-in production to explain this line was also considered

in Refs. [57,58]). It is problematic for N_1 produced by other mechanisms.

3.1 On the Higgs bosons

The analysis of the Higgs sector includes a theoretical constraint, i.e., the potential should be bounded from below (BFB) in order to make the minimum stable. We check this at tree level. It is more convenient to do so in the three-dimensional field space spanned by (h, J, σ), where the potential can be written as $V = X \Lambda X^T$ with $X = (h^2, J^2, \sigma^2)$ the bilinear vector and the matrix of coupling constants being

$$
\Lambda = \frac{1}{8} \begin{pmatrix} \lambda_h/3 & \lambda_{hJ} & \lambda_{h\sigma} \\ \lambda_{hJ} & \lambda_J/3 & \lambda_{J\sigma} \\ \lambda_{h\sigma} & \lambda_{J\sigma} & \lambda_\sigma/3 \end{pmatrix}. \tag{29}
$$

BFB requires that all of its sub-matrices $\Lambda_{n \times n}$ with $n = 1, 2, 3$ should satisfy the conditions $\mathrm{Tr}\,\Lambda_{n \times n} > 0$ and $\mathrm{Det}\,\Lambda_{n \times n} > 0$. Equivalently, the following conditions for the quartic couplings should be fulfilled:

$$
\begin{aligned}
&\lambda_h > 0, \quad \lambda_J > 0, \quad \lambda_\sigma > 0, \\
&|\lambda_{hJ}| < \frac{1}{3}\sqrt{\lambda_h \lambda_J}, \quad |\lambda_{h\sigma}| < \frac{1}{3}\sqrt{\lambda_h \lambda_\sigma}, \quad |\lambda_{J\sigma}| < \frac{1}{3}\sqrt{\lambda_J \lambda_\sigma}, \\
&|\lambda_h \lambda_{J\sigma}/3 - \lambda_{hJ}\lambda_{h\sigma}| < \sqrt{\lambda_h \lambda_J/9 - \lambda_{hJ}^2}\sqrt{\lambda_h \lambda_\sigma/9 - \lambda_{h\sigma}^2}.
\end{aligned} \tag{30}
$$

Basically, they require sufficiently small off-diagonal elements in Λ. Note that they practically lead to mass mixings in the Higgs mass matrix; thus the above conditions are consistent with the requirement that there should be a quite SM-like Higgs boson.

Aside from the renormalization scale Q, altogether the Higgs sector contains six real parameters, $\lambda_{h,\sigma,J}$ and $\lambda_{h\sigma}$, λ_{hJ}, $\lambda_{J\sigma}$. Among them, λ_h is almost fixed by the SM-like Higgs boson mass, and three can be expressed in terms of two VEV ratios x, y, and $\lambda_{h\sigma}$, $\lambda_{J\sigma}$. Since x and y have clear physical implications, they are taken to be inputs and fixed in our numerical samples. Finally, only three free parameters, λ_σ, $\lambda_{h\sigma}$, and $\lambda_{J\sigma}$, are left. We study the Higgs spectrum varying with them and display the results in Fig. 1, on the $\lambda_{h\sigma} - \lambda_{J\sigma}$ plane, with λ_σ chosen schematically. For each chosen λ_σ (dashed line), we show the corresponding mass spectrum through two lines, the thick line and dotted line for m_{H_2} and $m_{\mathcal{P}}$, respectively. For comparison, in Fig. 1 we show two choices of y: $y = 5$ (left panel) and $y = 3$ (right panel). Some observations are in order from the figure:

- In the singlet–doublet decoupling limit, $m_{h_{\mathrm{SM}}}$ in the expectation is merely sensitive to the diagonal quartic
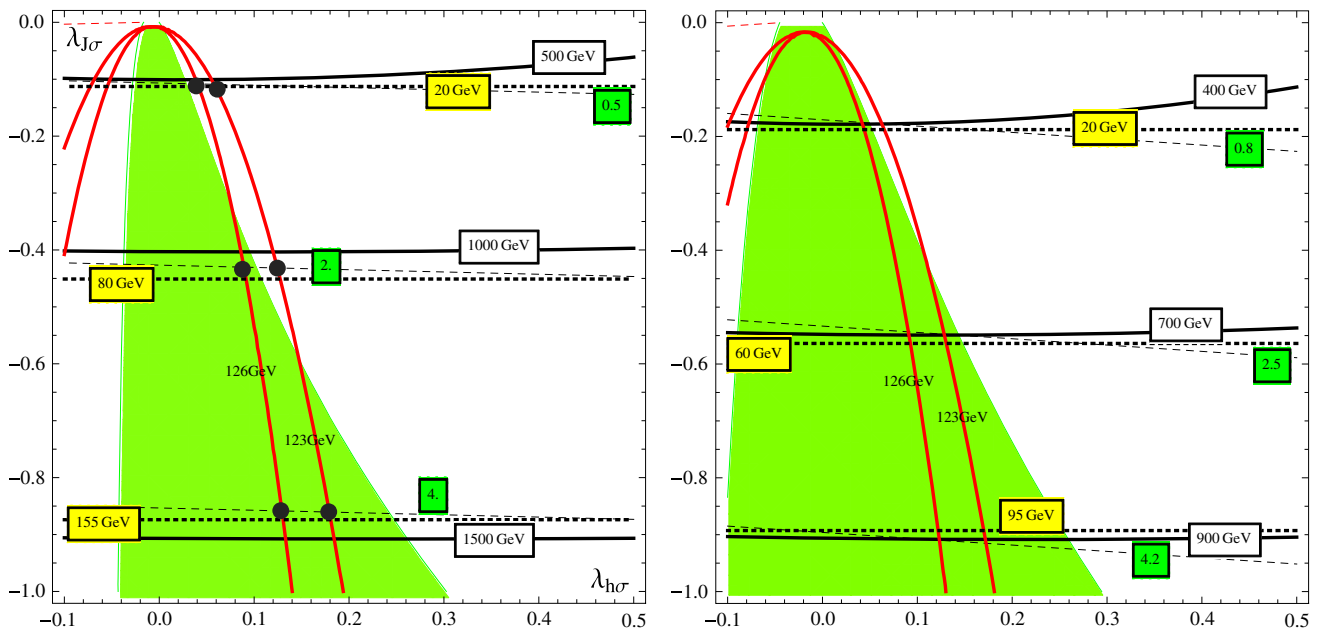
Fig. 1 *Left* contour plots of masses of the SM-like Higgs boson (*red thick lines*, two values 123 and 126 GeV taken), heaviest Higgs boson m_{H_2} (*black thick lines*) and PGSB (*dotted thick*). The *dashed lines* are for different choices of the values of λ_σ: 0.5, 2, 4. The *green-shadowed region* has been excluded by the BEFB condition. We take $y = 5$ and $x = 0.8$; $\lambda_h = 0.78$. *Right* the same but with $y = 3$ for comparison

coupling constant λ_h. Similarly, the masses of H_2 and $\mathcal{P}$ are sensitive to the diagonal quartic coupling constant in the singlet sector λ_σ but insensitive to the singlet–doublet mixing coupling constant $\lambda_{h\sigma}$.

- For all of the BEFB conditions listed in Eq. (30), practically the last one suffices. It excludes the regime outside the green-shadowed area. The intersection (black circle) between the Higgs mass- and λ_σ-curve is called a solution, determining a set of parameters $(\lambda_\sigma, \lambda_{h\sigma}, \lambda_{J\sigma}, \ldots)$. BEFB is able to rule out the smaller values of λ_σ for a larger $y(= 5)$, but for the smaller $y(= 3)$ this power tends to be lost. For illustration, in the $y = 5$ case we show three typical solutions with $\lambda_\sigma = 0.5, 2.0,$ and 4.0, respectively. One can see that given $m_{h_{SM}} = 123$–126 GeV, the first one has been excluded by BEFB, the second one is near exclusion, while the last one is safe.
- The region giving $m_{\mathcal{P}} < 114.4$ GeV is subject to the LEP constraint and $(m_{\mathcal{P}}, F_{\mathcal{P}h})$ are restricted. In turn, λ_σ and y are bounded. We do not intend to scan the whole parameter space since the studies of the SM Higgs doublet mixing with a singlet scalar have been done in many works, say, the most relevant one [43,44]. Generically, as long as λ_σ is around 1 and y is relatively large, $\mathcal{P}$ can easily avoid the LEP bound; if and only if y and λ_σ are of normal size, there is hope in the hunt for at least one of the two extra Higgs bosons. If in the future we do really hunt for two new Higgs bosons with hierarchical masses; the νSISM will be a good candidate to account for them.

3.2 On the FI*m*P with a benchmark at 3.5 keV X-ray line

Before heading toward the freeze-in production, we explain why N_1 with the DW mechanism has been ruled out already. N_1 can decay into a neutrino plus photon, with decay width [2]

$$\Gamma_{N_1 \to \nu\gamma} \simeq \frac{9 G_F^2 \alpha M_{N_1}^5}{256 \pi^4} \times \sum_\alpha \sin^2 \theta_{\alpha 1}, \tag{31}$$

where $\theta_{\alpha 1}$ is the mixing angle between N_1 and the active neutrino flavor ν_α. The nonobservation of an X-ray line stringently constrains on M_{N_1} and $\sum_\alpha \sin^2 \theta_{\alpha 1} \equiv \sin^2 \theta_1$ [59]. The width is proportional to $M_{N_1}^5$, so θ_1 is restricted to be very small for a heavier N_1. Consequently, the final yield of N_1 via the DW production is insufficient [2]:

$$\Omega_{\text{DW}} h^2 \approx 0.016 \times \left(\frac{\sin^2 \theta_1}{10^{-10}}\right) \left(\frac{M_{N_1}}{5\text{keV}}\right)^{1.8}. \tag{32}$$

Concretely, the region $M_{N_1} \gtrsim 3$–4 keV has been excluded. On the other hand, the Lyman-α (Lyα) forest gives a compensatory constraint on the lighter RHN which has a longer length of free streaming λ_{fs}. The latest analysis yields $M_{N_1} \gtrsim 8$ keV [60]. Therefore, the entire region of M_{N_1} has been excluded; see Fig. 2.

The DM production via freeze-in changes the situation dramatically. First, the X-ray bound can be avoided because
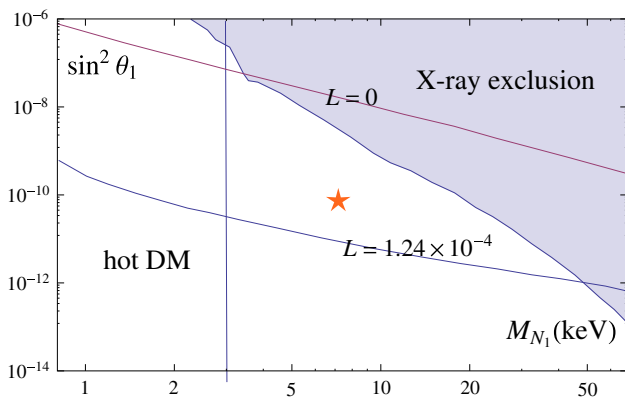
Fig. 2 In this plot, the *shadowed region* is excluded by the X-ray observations, and the *vertical line* at $M_{N_1} = 3$ keV indicates the lower bound on M_{N_1} from the free streaming limit. On the line with lepton asymmetry $L = 0$, a correct relic density of N_1 is achieved via the DW mechanism; while on the line with $L = 1.24 \times 10^{-4}$, it is via resonant production (we use data from Ref. [66]). The *red star* labels the point that fits the 3.55 keV X-ray anomaly. It lies in the bulk parameter space of the freeze-in scenario

the freeze-in production mechanism has nothing to do with the sterile-active neutrino mixing. In principle, it can be arbitrarily small given three families of RHN, because even in the limit of decoupling N_1 from the active neutrinos the other two heavy RHNs can still account for the neutrino masses and mixing.[7] Second, the Ly-α bound relaxes significantly because of two reasons. One is that $f(p, t)$, the initial spectrum of N_1, becomes slightly colder in the freeze-in scenario, where the average momentum of $f(p, t)$ is $\langle p_T \rangle \approx 2.45$ T, while in the DW scenario $\langle p_T \rangle \approx 2.8$ T [39]. The other one is due to a significant entropy dilution. Here N_1 is produced at the very early Universe t_{in}, corresponding to the temperature $T_{in} \simeq m_{H_a} \sim 0.1$–1 TeV. From t_{in} to the current time t_0 there is a large entropy release $\mathcal{S} \equiv g_*(t_{in})/g_*(t_0)$, which substantially cools N_1 down. Eventually, the average momentum becomes

$$\mathcal{S}^{-1/3} \langle p_T \rangle \approx \mathcal{S}^{-1/3} 2.45\, T. \tag{33}$$

The Ly-α bound accordingly weakens and merely gives $M_{N_1} > 1$ keV, a fairly loose bound. But to avoid a hot N_1 yields a stronger lower bound. In terms of Eq. (B4) the free streaming of N_1 is estimated to be[8]

---

[7] Such a limit amounts to the singlet fermionic FI*m*P via a singlet scalar portal [56]. Obviously, in that limit one does not need to worry about the *X*-ray bound.

[8] Different from the freeze-in scenario through a frozen-in scalar [37, 42], here the length of free streaming is independent on mass of the decaying scalar boson.

$$\lambda_{fs} = \mathcal{S}^{-1/3} \frac{\sqrt{a_{eq}}}{t_{eq}} \sqrt{t_{nr}} \left(5 + \ln \left(\frac{t_{eq}}{t_{nr}} \right) \right)$$
$$\simeq 0.038 \times \left(\frac{100}{g_*} \right)^{1/4} \left(\frac{10\text{keV}}{M_{N_1}} \right) \left(\frac{33}{\mathcal{S}} \right)^{1/3} \text{Mpc}, \tag{34}$$

where $\sqrt{t_{nr}}$ is the time at which RHN becomes nonrelativistic. To ensure that N_1 does not turn out to be hot, one requires $\lambda_{fs} \lesssim 0.1$ Mpc and in turn $M_{N_1} \gtrsim 3$ keV.

Interestingly, a X-ray line at energy 3.55 keV was recently reported with 3σ significance evidence [34, 35], through the observation of galaxy clusters and the Andromeda galaxy. Despite the controversy [61–64], it is tempting to interpret it as a smoking gun of decaying sterile neutrino with mass about 7.1 keV and mixing angle $\sin^2 2\theta_1 \approx 7 \times 10^{-11}$ [34, 35]. Production mechanisms of the correct relic density for such N_1 are relevant here. The non-resonant production fails already. The resonant production mechanism may work [65], but the latest work Ref. [38] showed that it also fails after taking into account the Ly-α bound. The freeze-in mechanism that gives a colder RHN, either via a frozen-in [37, 38] or a thermal scalar boson decay, successfully accommodates that N_1 with correct relic density in the bulk parameter space; see Fig. 2.

4 Conclusion and discussion

We proposed the FI*m*P framework for dark matter, a combination of FIMP with SI. It is consistent with the null results from all kinds of DM detections. Besides, it shows advantages in addressing basic questions about DM, stability, mass origin, and relic density generation, in an inherent way. In the golden example, the νSISM, the FI*m*P candidate, the lightest RHN N_1, furthermore is predicted instead of introduced artificially. We would like to stress that another attractive feature of the νSISM is its economy and self-consistence. Owing to scale invariance, it is necessary to incorporate extra singlets that develop VEVs around the TeV scale to generate Majorana masses for the RHNs. At the same time, they are capable of producing N_1 via freeze-in, addressing its relic density problem. It is not only so that these singlets are badly needed for SI spontaneously breaking itself.

Two open questions deserve further exploration. First, in this paper we actually work in the three RHNs scenario, so the X-ray bound is simply gone in the decoupling limit of N_1. But it is tempting to work in a more predictive framework where N_1 plays a more active role in neutrino physics, e.g., only two RHNs are introduced and then N_1's cannot decouple from active neutrinos. In that case, the resulting X-ray line will be closely correlated with neutrino phenomenologies. Second, it is of special interest to explore sterile neutrino DM in the scale invariant $B - L$ models [4, 67–70] where the RHNs have a more natural physical origin, i.e., they are required

by anomaly cancellation. But in such kinds of models RHNs carry $B - L$ charge and thus they are thermalized, except in the limit of decoupling new gauge dynamics, e.g., the new gauge coupling is vanishingly small or the massive gauge boson is very heavy, in such a way that it decouples before reheating.

Appendix A: The most general scalar potential: from complex to real

For the Higgs potential that consists of the SM Higgs doublet plus a complex singlet $S = (J + i\sigma)/\sqrt{2}$ and respects SI, the most general form reads

$$V_{\text{general}} = \frac{\lambda_1}{2}|H|^4 + \frac{\lambda_2}{2}|S|^4 + \lambda_3|H|^2|S|^2 \\ + \left(\lambda_4|H|^2S^2 + \lambda_5 S^3 S^* + \frac{\lambda_6}{2}S^4 + c.c.\right). \quad \text{(A1)}$$

It contains three real and three complex quartic coupling constants. One can also rewrite it in terms of the three real (physical) degrees of freedom, (h, J, σ):

$$V_{\text{general}} = \frac{\lambda_1}{8}h^4 + \frac{1}{4}\left(\frac{\lambda_2}{2} - 2\text{Re}\lambda_5 + \text{Re}\lambda_6\right)J^4 \\ + \frac{1}{4}\left(\frac{\lambda_2}{2} + 2\text{Re}\lambda_5 + \text{Re}\lambda_6\right)\sigma^4 \\ + \frac{1}{4}(\lambda_3 - 2\text{Re}\lambda_4)h^2J^2 + \frac{1}{4}(\lambda_3 + 2\text{Re}\lambda_4)h^2\sigma^2 \\ + \frac{1}{4}(\lambda_2 - 6\text{Re}\lambda_6)J^2\sigma^2 \\ - \text{Im}(\lambda_5 - \lambda_6)J^3\sigma - \text{Im}(\lambda_5 + \lambda_6)J\sigma^3 \\ - \text{Im}\lambda_4\,h^2J\sigma. \quad \text{(A2)}$$

Imposing CP-invariance on the Higgs sector forces the CP-odd part σ to appear in pairs and then terms in the last line disappear. In this sense, CP-invariance is equivalent to an Z_2 acting on σ. Of course, SI accidentally renders J and h charged under other accidental Z_2. Additionally, if we define

$$\lambda_h \equiv 3\lambda_1, \quad \lambda_J \equiv 3\lambda_2 - 12\lambda_5 + 6\text{Re}\lambda_6,$$
$$\lambda_\sigma \equiv 3\lambda_2 + 12\lambda_5 + 6\text{Re}\lambda_6, \quad \lambda_{hJ} \equiv \lambda_3 - 2\text{Re}\lambda_4,$$

$$\lambda_{h\sigma} \equiv \lambda_3 + 2\text{Re}\lambda_4, \quad \lambda_{J\sigma} \equiv \lambda_2 - 6\text{Re}\lambda_6,$$
$$\lambda_7 \equiv -6\text{Im}(\lambda_5 - \lambda_6), \quad \lambda_8 \equiv -6\text{Im}(\lambda_5 + \lambda_6),$$
$$\lambda_9 \equiv -2\text{Im}\lambda_4, \quad \text{(A3)}$$

the potential can be written as the form of $V = \lambda_{mml}h^n J^m \sigma^l / n!m!l!$ with $n + m + l = 4$.

Appendix B: Free streaming scale

A particle after decoupling from the thermal bath travels freely within the gravity potential. From the production time t_{in} of the particle to the present time t_0, which is far later than the matter radiation equality time scale $t_{\text{eq}} = 10^{11}s$, the mean free scale, i.e., the free streaming scale can be calculated via [42]

$$\lambda_{\text{fs}} = \int_{t_{\text{in}}}^{t_0} \frac{v(t)}{R(t)}\,dt = \int_{t_{\text{in}}}^{t_{\text{nr}}} \frac{1}{R(t)}\,dt \\ + \int_{t_{\text{nr}}}^{t_{\text{eq}}} \frac{v(t)}{R(t)}\,dt + \int_{t_{\text{nr}}}^{t_0} \frac{v(t)}{R(t)}\,dt. \quad \text{(B1)}$$

We have divided the integral into three regions. In the first region, the particle is relativistic and thus $v(t) = 1$. In the second and third regions the particle becomes nonrelativistic, with $v(t) = \langle p(t)\rangle/M_{N_1}$. During the radiation and matter dominating eras, the scale factor $R(t) = R_{\text{eq}}\sqrt{t/t_{\text{eq}}}$ and $R(t) = R_{\text{eq}}(t/t_{\text{eq}})^{2/3}$, respectively. Here t_{eq} and R_{eq} are the quantities defined at the radiation–matter equality. The critical time t_{nr} is determined by $\langle p(t)\rangle/M_{N_1} = 1$ with $\langle p(t)\rangle = 2.45T$, which gives

$$t_{\text{nr}} = 2.45^2 \times 0.3g_*^{-1/2}M_{\text{Pl}}/M_{N_1}^2 \\ \simeq 0.15 \times 10^5 \times \left(\frac{100}{g_*}\right)^{1/2}\left(\frac{10\text{keV}}{M_{N_1}}\right)^2 s, \quad \text{(B2)}$$

which justifies the assumption $t_{\text{nr}} \ll t_{\text{eq}} = 1.9 \times 10^{11}s$. Now, the nonrelativistic velocity is expressed as

$$v(t) = \sqrt{\frac{t_{\text{nr}}}{t}}, \quad (t_{\text{nr}} < t \leq t_{\text{eq}});$$
$$v(t) = \sqrt{\frac{t_{\text{nr}}}{t_{\text{eq}}}}\left(\frac{t_{\text{eq}}}{t}\right)^{2/3}, \quad (t > t_{\text{eq}}). \quad \text{(B3)}$$

With them, it is ready to calculate λ_{fs}:

$$\lambda_{\text{fs}} = \mathcal{S}^{-1/3}\frac{\sqrt{t_{\text{eq}}}}{R_{\text{eq}}}\left(2 + \ln\left(\frac{t_{\text{eq}}}{t_{\text{nr}}}\right) + 3\right)\sqrt{t_{\text{nr}}}. \quad \text{(B4)}$$

Note that t_{in} is at very early Universe, corresponding to temperature m_{H_a} around the weak scale; thus there is a sizable entropy dilution factor $\mathcal{S} \equiv g_*(t_{\text{in}})/g_*(t_0) \approx 33$, which

redshifts the momentum of dark matter by a factor $\mathcal{S}^{-1/3}$ as indicated above. It is not surprising that the above expression is the same as the one derived in Ref. [42], since the average momenta have the same scaling, behaving $\propto T$. The difference is manifest in the expression in t_{nr}.

Appendix C: Real scalar as a FImP

In this appendix we consider a scalar FImP S, which is supposed to be a real singlet scalar. Although it is not predicted by any well-motivated physics, it is still of great interest because of its even clearer way to show the main merits of FImP, stability, and common origins for mass and relic density.

Different from the RHN case, now it can directly couple to the SM Higgs doublet via $\lambda S^2 |H|^2 / 2$, which gives mass to the DM, $m_S = \sqrt{\lambda/2}v$. This realizes the toy model considered in Ref. [3], where only singlets are introduced with some of them triggering EWSB and the lightest one being a DM candidate. Here DM is not a WIMP but a FImP, thus viable for facing the strict direct detection bound. Concretely, in this single parameter model the freeze-in process is Higgs decaying into a pair of S, with decay width

$$\Gamma(h \to SS) = \frac{1}{32\pi} \frac{\lambda^2 v^2}{m_h}. \tag{C1}$$

Then the relic density, in terms of Eq. (21), is estimated to be

$$\Omega h^2 \simeq 0.12 \times \left(\frac{\lambda}{10^{-10.5}} \right)^{5/2} \left(\frac{v/m_h}{2.0} \right)^3 \left(\frac{10^3}{g_*^S \sqrt{g_*^\rho}} \right). \tag{C2}$$

But the DM mass is proportional to $\lambda^{1/2}$ instead of λ, thus DM now is predicted to be $m_S \simeq 1.0$ MeV. So this FImP is not warm DM-like (but it may elegantly account for a recent observation of DM self-interaction [71]). Varying the ratio v/m_h in an extended Higgs sector, for example, the two Higgs doublet model with the extra doublet H_2 developing a VEV around the GeV scale [3], the single term $\lambda_{12} S^2 \mathrm{Re}(H^\dagger H_2)$ may accommodate the scalar FImP as warm DM again.

References

1. D. Akerib et al., LUX Collaboration (2013). arXiv:1310.8214
2. A. Kusenko, Phys. Rep. **481**, 1 (2009). arXiv:0906.2968
3. J. Guo, Z. Kang, Nucl. Phys. B **898**, 415 (2015)
4. J. Guo, Z. Kang, P. Ko, Y. Orikasa, Phys. Rev. D **91**(11), 115017 (2015)
5. W.A. Bardeen, FERMILAB-CONF-95-391-T, C95-08-27.3 (1995)
6. R. Hempfling, Phys. Lett. B **379**, 153 (1996)
7. K.A. Meissner, H. Nicolai, Phys. Lett. B **648**, 312 (2007)
8. W.-F. Chang, J.N. Ng, J.M.S. Wu, Phys. Rev. D **75**, 115016 (2007)
9. R. Foot, A. Kobakhidze, R.R. Volkas, Phys. Lett. B **655**, 156 (2007)
10. R. Foot, A. Kobakhidze, K.L. McDonald, R.R. Volkas, Phys. Rev. D **77**, 035006 (2008)
11. R. Foot, A. Kobakhidze, K.L. McDonald, R.R. Volkas, Phys. Rev. D **76**, 075014 (2007)
12. S. Iso, N. Okada, Y. Orikasa, Phys. Rev. D **80**, 115007 (2009)
13. S. Iso, N. Okada, Y. Orikasa, Phys. Lett. B **676**, 81 (2009)
14. M. Holthausen, M. Lindner, M.A. Schmidt, Phys. Rev. D **82**, 055002 (2010)
15. C. Englert, J. Jaeckel, V.V. Khoze, M. Spannowsky, JHEP **1304**, 060 (2013)
16. C. Englert, J. Jaeckel, V.V. Khoze, M. Spannowsky, Phys. Rev. D **88**, 055020 (2013)
17. M. Lindner, S. Schmidt, J. Smirnov. arXiv:1405.6204
18. R. Dermisek, T.H. Jung, H.D. Kim. arXiv:1308.0891
19. C. Tamarit, Phys. Rev. D **90**, 055024 (2014)
20. T. Hambye, M.H.G. Tytgat, Phys. Lett. B **659**, 651 (2008)
21. T. Hambye, A. Strumia, Phys. Rev. D **88**, 055022 (2013)
22. V.V. Khoze, JHEP **1311**, 215 (2013)
23. E. Gabrielli, M. Heikinheimo, K. Kannike, A. Racioppi, M. Raidal, C. Spethmann, Phys. Rev. D **89**, 015017 (2014)
24. S. Benic, B. Radovcic, Phys. Lett. B **732**, 91 (2014)
25. T. Hur, D.-W. Jung, P. Ko, J.Y. Lee, Phys. Lett. B **696**, 262 (2011)
26. T. Hur, P. Ko, Phys. Rev. Lett. **106**, 141802 (2011)
27. M. Heikinheimo, A. Racioppi, M. Raidal, C. Spethmann, K. Tuominen. arXiv:1304.7006
28. Durmus A. Demir, Mariana Frank, Beste Korutlu, Phys. Lett. B **728**, 393–399 (2014)
29. M. Holthausen, J. Kubo, K.S. Lim, M. Lindner, JHEP **1312**, 076 (2013)
30. M. Heikinheimo, C. Spethmann, JHEP **1412**, 084 (2014)
31. O. Antipin, M. Redi, A. Strumia. arXiv:1410.1817 [hep-ph]
32. J. McDonald, Phys. Rev. Lett. **88**, 091304 (2002)
33. L.J. Hall, K. Jedamzik, J. March-Russell, S.M. West, JHEP **1003**, 080 (2010). arXiv:0911.1120
34. E. Bulbul, M. Markevitch, A. Foster, R.K. Smith, M. Loewenstein, S.W. Randall. arXiv:1402.2301
35. A. Boyarsky, O. Ruchayskiy, D. Iakubovskyi, J. Franse. arXiv:1402.4119
36. M. Frigerio, C.E. Yaguna. arXiv:1409.0659 [hep-ph]
37. A. Adulpravitchai, M.A. Schmidt. arXiv:1409.4330 [hep-ph]
38. A. Merle, A. Schneider. arXiv:1409.6311 [hep-ph]
39. M. Shaposhnikov, I. Tkachev, Phys. Lett. B **639**, 414 (2006)
40. A. Kusenko, Phys. Rev. Lett. **97**, 241301 (2006)
41. K. Petraki, A. Kusenko, Phys. Rev. D **77**, 065014 (2008)
42. A. Merle, V. Niro, D. Schmidt, JCAP **1403**, 028 (2014). arXiv:1306.3996 [hep-ph]
43. A. Farzinnia, H.-J. He, J. Ren. arXiv:1308.0295
44. A. Farzinnia, J. Ren, Phys. Rev. D **90**, 015019 (2014)
45. L. Alexander-Nunneley, A. Pilaftsis, JHEP **1009**, 021 (2010)
46. E. Gildener, S. Weinberg, Phys. Rev. D **13**, 3333 (1976)
47. S. Coleman, E. Weinberg, Phys. Rev. D **7**, 1888 (1973)
48. S. Dodelson, L.M. Widrow, Phys. Rev. Lett. **72**, 17–20 (1994). arXiv:hep-ph/9303287
49. X.-D. Shi, G.M. Fuller, Phys. Rev. Lett. **82**, 2832 (1999). arXiv:astro-ph/9810076
50. F. Bezrukov, H. Hettmansperger, M. Lindner, Phys. Rev. D **81**, 085032 (2010)
51. D.H. Weinberg, J.S. Bullock, F. Governato, R.K. de Naray, A.H.G. Peter. arXiv:1306.0913 [astro-ph.CO]
52. X. Chu, T. Hambye, M.H.G. Tytgat, JCAP **1205**, 034 (2012)
53. P.S. Bhupal Dev, A. Mazumdar, S. Qutub, Front. Phys. **2**, 26 (2014)
54. F. Elahi, C. Kolda, J. Unwin. arXiv:1410.6157 [hep-ph]

55. Z. Kang, T. Li, JHEP **1102**, 035 (2011). arXiv:1008.1621 [hep-ph]
56. M. Klasen, C.E. Yaguna, JCAP **1311**, 039 (2013). arXiv:1309.2777 [hep-ph]
57. E. Dudas, L. Heurtier, Y. Mambrini, Phys. Rev. D **90**, 035002 (2014)
58. C. Kolda, J. Unwin, Phys. Rev. D **90**, 023535 (2014)
59. K. Abazajian, S.M. Koushiappas, Phys. Rev. D **74**, 023527 (2006). arXiv:astro-ph/0605271
60. M. Viel, G.D. Becker, J.S. Bolton, M.G.A. Haehnelt, Phys. Rev. D **88**, 3502 (2013)
61. T.E. Jeltema, S. Profumo. arXiv:1408.1699
62. D. Malyshev, A. Neronov, D. Eckert. arXiv:1408.3531
63. A. Boyarsky, J. Franse, D. Iakubovskyi, O. Ruchayskiy. arXiv:1408.4388
64. E. Bulbul, M. Markevitch, A.R. Foster, R.K. Smith, M. Loewenstein, S.W. Randall. arXiv:1409.4143
65. K.N. Abazajian. arXiv:1403.0954
66. L. Canetti, M. Drewes, T. Frossard, M. Shaposhnikov, Phys. Rev. D **87**(9), 093006 (2013). arXiv:1208.4607 [hep-ph]
67. V.V. Khoze, G. Ro, JHEP **1310**, 075 (2013)
68. C.D. Carone, R. Ramos, Phys. Rev. D **88**, 055020 (2013)
69. E.J. Chun, S. Jung, H.M. Lee, Phys. Lett. B **725**, 158 (2013)
70. H. Okada, Y. Orikasa. arXiv:1412.3616 [hep-ph]
71. Z. Kang. arXiv:1505.06554 [hep-ph]